Elimination of single-beam substitution error in diffuse reflectance measurements using an integrating sphere

Luka Vidovič
Boris Majaron

Elimination of single-beam substitution error in diffuse reflectance measurements using an integrating sphere

Luka Vidovič* and Boris Majaron
Jožef Stefan Institute, Jamova 39, SI-1000 Ljubljana, Slovenia

Abstract. Diffuse reflectance spectra (DRS) of biological samples are commonly measured using an integrating sphere (IS). To account for the incident light spectrum, measurement begins by placing a highly reflective white standard against the IS sample opening and collecting the reflected light. After replacing the white standard with the test sample of interest, DRS of the latter is determined as the ratio of the two values at each involved wavelength. However, such a substitution may alter the fluence rate inside the IS. This leads to distortion of measured DRS, which is known as single-beam substitution error (SBSE). Barring the use of more complex experimental setups, the literature states that only approximate corrections of the SBSE are possible, e.g., by using look-up tables generated with calibrated low-reflectivity standards. We present a practical method for elimination of SBSE when using IS equipped with an additional reference port. Two additional measurements performed at this port enable a rigorous elimination of SBSE. Our experimental characterization of SBSE is replicated by theoretical derivation. This offers an alternative possibility of computational removal of SBSE based on advance characterization of a specific DRS setup. The influence of SBSE on quantitative analysis of DRS is illustrated in one application example. © 2014 Society of Photo-Optical Instrumentation Engineers (SPIE) [DOI: 10.1117/1.JBO.19.2.027006]

Keywords: diffuse reflectance spectroscopy; integrating sphere; single-beam substitution error; skin characterization.

Paper 130754PR received Oct. 17, 2013; revised manuscript received Dec. 5, 2013; accepted for publication Jan. 20, 2014; published online Feb. 18, 2014.

1 Introduction

Diffuse reflectance spectroscopy in visible and near-infrared part of the spectrum is a popular experimental technique in biomedical optics. Quantitative comparisons of measured diffuse reflectance spectra (DRS) with theoretical predictions were used, e.g., to determine various tissue optical properties.[1–6] In addition, several groups have applied DRS for analysis of spatially heterogeneous organs, such as human skin,[7–9] with specific aims to assess concentrations of epidermal melanin[10–12] or other skin chromophores,[13–15] enable diagnostic characterization of skin lesions,[16–18] or monitor time evolution of traumatic bruises.[19–21]

A common setup for diffuse reflectance spectroscopy involves an integrating sphere (IS) with internal broadband light source. The IS is a spherical cavity with a highly reflective coating, which provides evenly distributed illumination of the sample, placed at the circular sample opening. A built-in lens focuses a narrow pencil of light reflected from the central part of the sample into an optical fiber attached to the IS signal port to transmit the collected light to an external spectrometer.

In order to account for illumination spectrum, each DRS measurement session begins by acquiring a spectrum of light reflected off a highly reflective white standard material. After replacing the white standard with sample of interest, DRS of the latter is determined by dividing the two spectra at each involved wavelength. However, the substitution of the white standard for the sample may alter the light fluence inside the IS. This effect can cause a distortion of measured DRS, which is known as the single-beam substitution error (SBSE).

The existence of SBSE is acknowledged in the scientific literature[22–24] and some manufacturers' white papers.[25–27] However, the error is usually claimed to be small (i.e., below a few percent) and is, thus, commonly neglected.[25] For applications that require accurate diffuse reflectance values, use of dedicated IS equipped with an additional dummy port or even more complex dual-beam experimental setups is suggested to eliminate the SBSE. When such equipment is unavailable or would be too impractical to use, the literature states that only approximate compensation for the SBSE is possible, e.g., by using a look-up table prepared with a set of lower reflectivity gray standards.[24,25]

In the following, we present a few practical methods for elimination of SBSE when using IS equipped with an additional reference port. This allows monitoring of light field inside the IS and, thus, enables rigorous elimination of the SBSE based on two additional calibration measurements. In the presented experimental examples performed using a rather popular experimental setup, the presence of SBSE leads to significantly underestimated and somewhat distorted DRS.

Our experimental observations are replicated by predictions based on a theoretical derivation. This offers the possibility to compensate for SBSE based on advance characterization of a specific DRS setup, thus effectively eliminating the need to perform any additional calibration measurements during the actual application.

2 Measurement of DRS Using an Integrating Sphere

Let us consider an IS with the signal port located at a small angle ϑ with respect to the sample normal (see Fig. 1). A lens

---

*Address all correspondence to: Luka Vidovič, E-mail: luka.vidovic@ijs.si
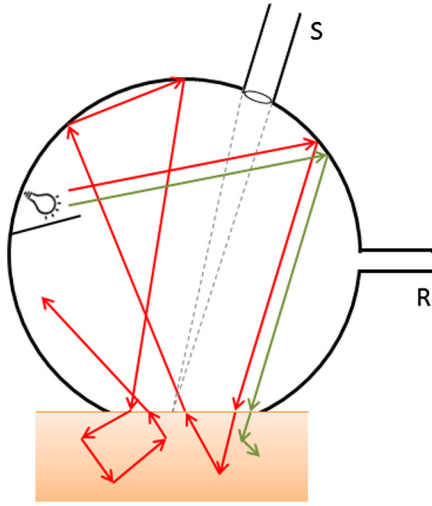
Fig. 1 Scheme of an integrating sphere with internal light source. S, signal port; R, reference port. The irradiation spectrum is represented by two wavelengths (red and green arrows, respectively) with different absorption and scattering properties inside the sample material.

positioned at the signal port collects light reflected from a small sample area A_0 within a spatial angle $\Delta\Omega$ onto the end of an optical fiber inserted into the port (not depicted). The signal passed to the external spectrometer is, thus, related to sample radiance, $L_{\text{sam}}(\lambda)$, as

$$S_{\text{sam}}(\lambda) = A_0 \cos\vartheta \Delta\Omega L_{\text{sam}}(\lambda). \tag{1}$$

Under the even irradiation provided by the IS and assuming a Lambertian sample surface, radiance of the latter is isotropic and linked to sample diffuse reflectivity (R_{sam}) as

$$L_{\text{sam}}(\lambda) = \frac{1}{2\pi}\phi(\lambda)R_{\text{sam}}(\lambda), \tag{2}$$

where $\phi(\lambda)$ represents spectral distribution of the incident fluence rate. Consequently, the detected spectrum can be expressed as

$$S_{\text{sam}}(\lambda) = \alpha\,\phi(\lambda)R_{\text{sam}}(\lambda), \tag{3}$$

where all spectrally independent terms were lumped into a single constant, $\alpha = A_0 \cos\vartheta \Delta\Omega/(2\pi)$.

Following the manufacturers' instructions,[28–30] measurements of DRS begin by recording one spectrum with the internal light source turned off and the sample port covered. The obtained dark spectrum represents the baseline (noise) values, which are automatically subtracted from all subsequent measurements. In the interest of clarity, we will not account for this trivial step in the following expressions.

Next, the measurement proceeds by placing a highly reflective white standard at the sample opening and recording the so-called white spectrum, $S_{\text{wh}}(\lambda)$.

Finally, the white standard can be replaced with the sample of interest. Its DRS is determined by dividing, at each involved wavelength, the recorded sample spectrum values, $S_{\text{sam}}(\lambda)$, with the corresponding white spectrum values.

$$R'(\lambda) = \frac{S_{\text{sam}}(\lambda)}{S_{\text{wh}}(\lambda)} = \frac{\phi_{\text{sam}}(\lambda)R_{\text{sam}}(\lambda)}{\phi_{\text{wh}}(\lambda)R_{\text{wh}}(\lambda)}. \tag{4}$$

Here, $\phi_{\text{sam}}(\lambda)$ and $\phi_{\text{wh}}(\lambda)$ represent the spectrally resolved fluence rates inside the IS when acquiring the signals from the sample or white standard, respectively.

As is evident from Eq. (4), the main rationale behind the described procedure is that specifics of light fluence inside the IS will not influence the result, provided that the former is not being affected upon the substitution of white standard with the sample. Under this assumption, $R'(\lambda)$ matches $R_{\text{sam}}(\lambda)$ as long as the white standard reflectivity (R_{wh}) equals 1 across the involved spectral range. Most commercial spectrometers of the discussed type report the obtained spectral ratio $R'(\lambda)$ as the sample's DRS, thereby tacitly implying that both above-stated assumptions are valid.

Within the visible and near-infrared spectral range, high-quality white standards with $R_{\text{wh}} = 0.99$ or higher are readily available. As indicated by Eq. (4), the relative error induced by deviation of R_{wh} from the ideal value of 1 will be proportional to that difference and, thereby, usually <1%. Moreover, the related error can be easily removed by applying manufacturer-provided data on $R_{\text{wh}}(\lambda)$ and Eq. (4).

2.1 Single-Beam Substitution Error

Because IS is essentially a diffuse optical resonator, the fluence rate inside it depends on both radiant power and spectrum of the internal light source, as well as reflectivity of its walls—and also of the material placed at the sample opening. Consequently, $\phi(\lambda)$ will in principle be affected by the substitution of white standard with the sample, as soon as sample reflectivity $R_{\text{sam}}(\lambda)$ differs from $R_{\text{wh}}(\lambda)$ anywhere within the involved spectral band.

The effect is illustrated in Fig. 1, where light field inside the IS is represented by two spectral components, which experience different absorption and scattering properties of the sample tissue. As some of the incident radiant power undergoes selective absorption inside the sample, or leaves its surface outside of the sample opening, the amount of light re-emitted into the IS will, in general, be spectrally varied. Moreover, it will be different from that induced by the highly reflective white standard.

As indicated by Eq. (4), any significant difference between $\phi_{\text{sam}}(\lambda)$ and $\phi_{\text{wh}}(\lambda)$ will lead to deviation of the spectrometer-reported proxy value $R'(\lambda)$ from the actual sample reflectance, $R_{\text{sam}}(\lambda)$. This artifact is known as SBSE.[22–27]

In applications that require accurate values of $R_{\text{sam}}(\lambda)$, it is advisable to check for presence of SBSE and—if it turns out to be significant—correct for it before using experimental data in subsequent quantitative analysis.

3 Experimental Characterization and Elimination of SBSE

In Fig. 2, we present an example of the customary DRS measurement procedure, as described above. The data were obtained using an IS with internal light source and a spectrometer sensitive in the 400- to 1000-nm spectral range (ISP-REF and USB4000, respectively, by Ocean Optics, Dunedin, Florida). For the white standard, we used optical-grade Spectralon® (by Labsphere, North Sutton, New Hampshire) with Lambertian reflectance of $R_{\text{wh}} \geq 0.99$ at 400 to 1500 nm.[31]
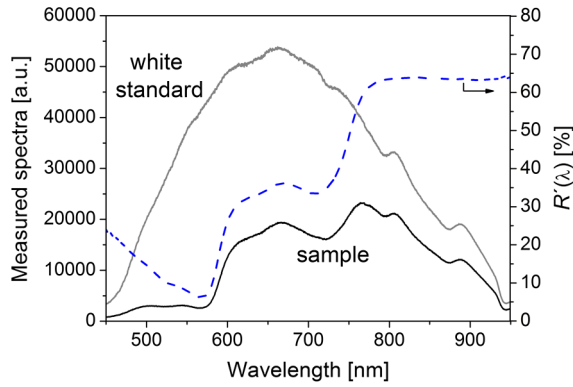
Fig. 2 Spectra measured at the integrating sphere (IS) signal port for the white standard (gray line) and our test sample (black line). Dashed line (blue) represents the approximate diffuse reflectance spectra (DRS) of the latter, $R'(\lambda)$.

The spectrally resolved signal as collected from the white standard, $S_{wh}(\lambda)$ is indicated by the solid gray line. The black line marks the spectrum obtained from our test sample, $S_{sam}(\lambda)$. In order to ensure good reproducibility, the test sample was an orange cardboard. The ratio of the two spectra, $R'(\lambda)$, which the spectrometer software (SpectraSuite, Ocean Optics) reports as the sample DRS, is presented by the dashed line (blue).

Our analysis of SBSE utilizes the so-called reference port, which is provided on the specified IS in addition to the signal port (see Fig. 1). In contrast with the latter, the reference port always collects light reflected from the IS walls. By analogy with Eq. (3), signals collected at this port, thus, equal

$$S^R(\lambda) = \beta \, \phi(\lambda) \rho(\lambda), \tag{5}$$

where β accounts for optical properties of the reference port, and $\rho(\lambda)$ stands for diffuse reflectivity of the IS walls.

Since both β and $\rho(\lambda)$ will be constant throughout the measurement session, $S^R(\lambda)$ can vary only in response to potential changes of fluence rate inside the IS, $\phi(\lambda)$. Thus, measurements performed at this port enable us to check for alteration of $\phi(\lambda)$ upon the substitution of white standard with the sample.
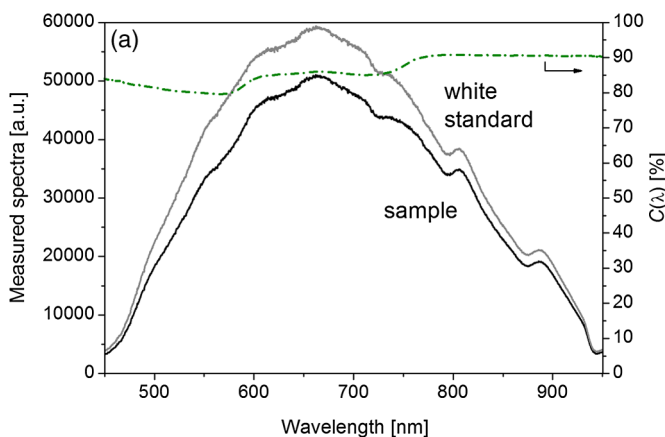
The result of such a test, performed with our orange cardboard sample, shows that the two reference spectra $S^R(\lambda)$ are indeed markedly different [Fig. 3(a)]. By performing the two measurements in the same way as described above, the spectrometer software reports the ratios of the corresponding spectral values.

$$C(\lambda) = \frac{S_{sam}^R(\lambda)}{S_{wh}^R(\lambda)} = \frac{\phi_{sam}(\lambda)}{\phi_{wh}(\lambda)}. \tag{6}$$

The result (green, dash-dotted line) reveals that within the involved spectral range, the relative change of $\phi(\lambda)$ amounts to 9 to 20%.

3.1 Elimination of SBSE—Experimental Approach

Quantitative characterization of the fluence rate alteration inside the IS, as provided by our additional measurements performed at the reference port, enables us to rigorously eliminate the SBSE from the provisional DRS, $R'(\lambda)$ [Eq. (4)]. Namely, dividing the latter with the corresponding correction terms $C(\lambda)$ [Eq. (6)] at each involved wavelength yields exactly

$$R''(\lambda) = \frac{R'(\lambda)}{C(\lambda)} = \frac{R_{sam}(\lambda)}{R_{wh}(\lambda)}. \tag{7}$$

The corrected DRS spectrum, $R''(\lambda)$, is thus free from SBSE. Its amplitude and shape match the sample reflectance $R_{sam}(\lambda)$, inasmuch as $R_{wh} = 1$.

In Fig. 3(b), we compare the provisional DRS of our test sample, $R'(\lambda)$ (dashed line), with the spectrum corrected according to Eq. (7) (solid). The result demonstrates that the former values are significantly underestimated over the entire spectral range.

A more complete characterization of SBSE is presented in Fig. 4. Here, one white and one orange paper sheet were used as test samples in order to cover a wider range of diffuse reflectance values. DRS as obtained for both samples with and without the elimination of SBSE are compared in Fig. 4(a) (solid and dashed lines, respectively). This allows us to experimentally assess the artifact due to SBSE, i.e., $\Delta_{SBS}(\lambda) = R'(\lambda) - R'(\lambda)$. The obtained values are plotted in Fig. 4(b) as a function of the
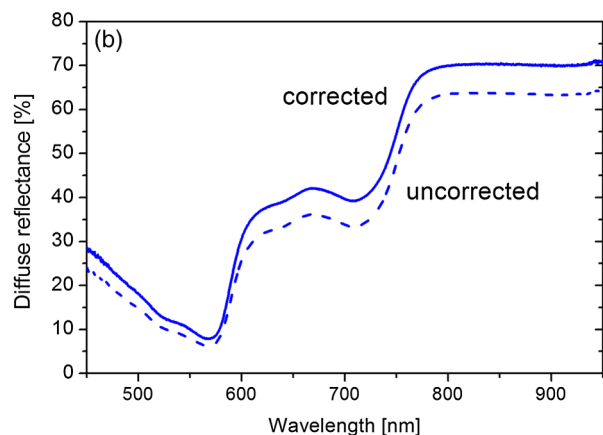
Fig. 3 (a) Spectra $S^R(\lambda)$ as measured at the IS reference port for the white standard (gray line) and our test sample (black). The dash-dotted line indicates their ratio, $C(\lambda)$. (b) DRS of our sample as obtained with (solid line) and without (dash) elimination of single-beam substitution error (SBSE) according to Eq. (7).
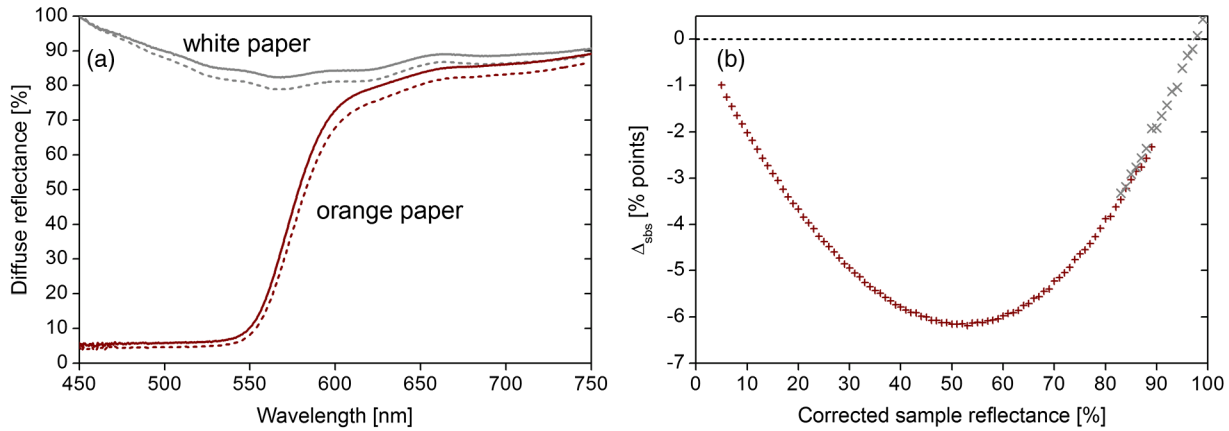
Fig. 4 (a) DRS of white (gray lines) and orange paper (black), as obtained with and without elimination of the SBSE (solid and dashed lines, respectively). (b) Amplitude of the SBSE as a function of the corrected sample reflectance, R'', as assessed from data in Fig. 4(a).

corresponding values R'', which are close to the actual sample reflectance R_{sam} at the respective wavelength [see Eq. (7)].

The result suggests that Δ_{SBS} is a unique, albeit highly non-linear function of the sample reflectance. For the discussed experimental setup, Δ_{SBS} exceeds 6 percentage points at sample reflectance values between 40 and 65%. Consequently, the provisional reflectance values R' exhibit relative errors that amount up to 17%.

3.2 Experimental Elimination of SBSE—an Alternative Approach

The described experimental procedure, while conceptually clear, can be somewhat impractical when measurements involve test animals or human volunteers. Obtaining each SBSE-free DRS namely involves acquisition of four raw spectra, two substitutions of white standard with sample of interest, and one repositioning of the optical fiber from the signal port to the reference port at midpoint. All this must be performed in presence of test subjects, thereby prolonging the measurement protocol and potentially introducing additional artifacts, e.g., due to inaccurate repositioning of the IS at the test site.

In order to alleviate the above drawbacks, we propose an alternative procedure for measurement of SBSE-free DRS. In this approach, two measurements at the sample of interest are performed consecutively, with the optical fiber positioned at the sample and reference port of the IS, respectively. According to Eqs. (3) and (5), the ratio of acquired spectra, reported by the spectrometer software, equals

$$\tilde{R}(\lambda) = \frac{\alpha}{\beta} \frac{R_{sam}(\lambda)}{\rho(\lambda)}. \tag{8}$$

Note that this procedure does not involve the substitution of the sample with white standard, so the fluence rate inside the IS does not change between the two measurements. Strictly speaking, the concept of SBSE does not apply in this situation. Inasmuch as $\rho(\lambda)$ equals 1, the obtained spectrum $\tilde{R}(\lambda)$ is, thus, exactly proportional to sample reflectivity, $R_{sam}(\lambda)$. However, the two are related by an unknown factor, α/β.

Because optical properties of the two IS ports are constant throughout the measurement session, this factor can be determined by a separate calibration measurement. This measurement

also involves repositioning of the optical fiber from the sample port to the reference port, with the white standard placed at the sample opening. In analogy with Eq. (8), the ratio between the obtained spectra is

$$\tilde{C}(\lambda) = \frac{\alpha}{\beta} \frac{R_{wh}(\lambda)}{\rho(\lambda)}. \tag{9}$$

Dividing $\tilde{R}(\lambda)$ with the port calibration factor $\tilde{C}(\lambda)$ evidently eliminates the factor α/β, as well as spectral reflectivity of the IS walls, $\rho(\lambda)$, to yield the SBS-free DRS.

$$\frac{\tilde{R}(\lambda)}{\tilde{C}(\lambda)} = \frac{R_{sam}(\lambda)}{R_{wh}(\lambda)} = R''(\lambda). \tag{10}$$

The obtained result is identical to that in Eq. (7). This is not surprising because both procedures involve the same four measurements, only combined in a slightly different way.

Nevertheless, this alternative approach has an important practical advantage in that each pair of sample measurements, necessary to determine $\tilde{R}(\lambda)$, is performed successively. Consequently, they can be performed without repositioning of the IS and a minimal time interval between them. This should reduce patient or animal discomfort and their time spent in the lab—or alternatively, increase the number of test sites that can be investigated within the available time interval.

In addition, because the port calibration term $\tilde{C}(\lambda)$ does not depend on sample specifics or vary with time, it can be assessed only once for the entire measurement session, thus also reducing the total operator time. Moreover, since this measurement involves only the white standard, a significantly longer signal acquisition time can be used, thus enabling more accurate determination of $\tilde{C}(\lambda)$ due to increased signal-to-noise ratio. This is a clear advantage over the measurements of $R'(\lambda)$ and $C(\lambda)$ in the former approach, where signal acquisition time is often limited by risks related to heating of sample tissue with the IS light. These risks include, e.g., measurement artifacts due to uncontrolled physiological responses, adverse side effects in animal or human subjects, and thermal damaging of *ex vivo* tissue samples.

4 Theoretical Analysis

Inside the IS, light emitted from the internal source of power $P(\lambda)$ is multiply reflected from its walls with a total surface area A and spectral reflectance $\rho(\lambda)$. The fraction of light lost through the IS openings (e.g., signal and reference ports, sample opening) is proportional to their combined fractional area, F. However, at the sample opening (with fractional area f), light is partially reflected back into the IS, depending on sample reflectivity $R_{sam}(\lambda)$.

Radiometric treatment of the above situation yields an analytical expression for radiance of the sample surface positioned at the IS sample opening[32]

$$L_{sam}(\lambda) = \frac{P(\lambda)}{\pi A} \frac{R_{sam}(\lambda)}{[1 - (1 - F)\rho(\lambda) - fR_{sam}(\lambda)]}. \quad (11)$$

By using Eq. (1) and our definition of α, the spectrum measured at the signal port can thus be written as

$$S_{sam}(\lambda) = \alpha R_{sam}(\lambda) \frac{2P(\lambda)}{A[1 - (1 - F)\rho(\lambda) - fR_{sam}(\lambda)]}. \quad (12)$$

A comparison with Eq. (3) tells us that the last term matches $\phi_{sam}(\lambda)$.

The spectrum obtained when the sample is replaced with the white standard is analogous to Eq. (12), with $R_{sam}(\lambda)$ substituted by $R_{wh}(\lambda)$. The provisional DRS, as obtained by the customary measurement procedure, therefore, equals [see Eq. (4)]

$$R'(\lambda) = \frac{R_{sam}(\lambda)}{R_{wh}(\lambda)} \left[\frac{1 - (1 - F)\rho(\lambda) - fR_{wh}(\lambda)}{1 - (1 - F)\rho(\lambda) - fR_{sam}(\lambda)} \right]. \quad (13)$$

By comparison with Eq. (4), we can see that the SBSE occurs when the bracketed fraction in Eq. (13) deviates from the value of 1. The provided expression shows very clearly how this arises from inevitable differences between $R_{sam}(\lambda)$ and $R_{wh}(\lambda)$.

Similar to the white standard, $\rho(\lambda)$ is usually very high and exhibits a weak spectral dependence. In the IS used in our experimental example, the cavity walls are covered with Spectralon®, the same material as used for the white standard. Within the discussed spectral range, its reflectivity is practically constant, $\rho = R_{wh} = 0.991 \pm 0.001$.[33] This simplifies the expression for measurement artifact due to SBSE.

$$\Delta_{SBS}(\lambda) = R'(\lambda) - R''(\lambda)$$
$$= \frac{R_{sam}(\lambda)}{R_{wh}} \left[\frac{1 - (1 - F)\rho - fR_{wh}}{1 - (1 - F)\rho - fR_{sam}(\lambda)} - 1 \right]. \quad (14)$$

The wavelength dependence of Δ_{SBS}, thus, arises exclusively from $R_{sam}(\lambda)$. Consequently, Δ_{SBS} becomes a unique function of R_{sam}.

The result is presented in Fig. 5. From the diameters of our IS cavity (38.1 mm)[33] and sample opening (10.3 mm), we obtain $f = 0.018$. Setting the fractional area of all openings combined (undocumented) to $F = 0.07$—a reasonable value given the IS structure—results in an excellent match of the function's shape and amplitude with our experimental data [Fig. 4(b)]. As can be seen from Eq. (14), Δ_{SBS} becomes positive when R_{sam} exceeds R_{wh}.

Equation (14) also provides an insight into quantitative relations between the relevant properties of the IS and the SBSE. The expression is rather involved, but the gross behavior can
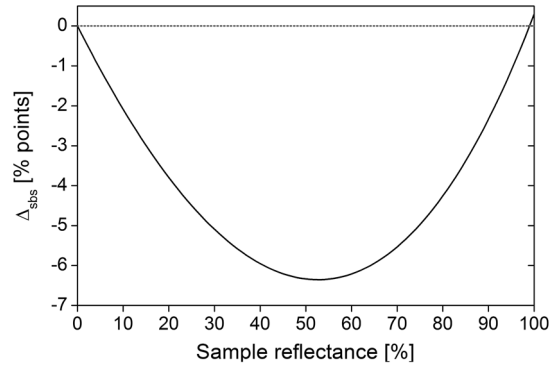
Fig. 5 SBSE as calculated from Eq. (14) for an integrating sphere with $\rho = R_{wh} = 0.991$, $f = 0.018$, and $F = 0.07$.

be assessed from its approximate form, obtained by setting $\rho = R_{wh} = 1$.

$$\Delta_{SBS} \approx -f \frac{R_{sam}(1 - R_{sam})}{F - fR_{sam}}. \quad (15)$$

In most realistic examples, we will have $F > fR_{sam}$, which makes the denominator in Eq. (15) rather stationary. Consequently, Δ_{SBS} will exhibit a nearly parabolic dependence on R_{sam} (see Fig. 5), with the amplitude roughly proportional to f. In practical terms, this means that SBSE will be more pronounced in IS with larger sample openings. On the other hand, increasing the IS cavity diameter while keeping everything else the same will reduce the value of f and, thereby, also Δ_{SBS}.

4.1 Computational Elimination of SBSE

The good match between our experimental characterization of SBSE [Fig. 4(b)] and theoretical prediction based on Eq. (14) (see Fig. 5) offers yet another possibility for correction of DRS, as obtained by the customary measurement procedure.

The first step of this approach involves determination of the function that describes best the characteristics of SBSE in a specific instrument. By using Eq. (14), this pertains, in particular, to finding the optimal value of parameter F. This task can be easily performed by each end user by following the steps described in the present article (see Fig. 4) and using the parameter values (f, ρ, and R_{wh}) appropriate for their own equipment.

For the second step, we use the identity $R_{sam}(\lambda) = R_{wh} R''(\lambda)$ [Eq. (7)] to rewrite Eq. (14) as

$$R'(\lambda) = R''(\lambda) \frac{1 - (1 - F)\rho - fR_{wh}}{1 - (1 - F)\rho - fR_{wh}R''(\lambda)}. \quad (16)$$

By applying some basic algebra (but no additional assumptions or approximations), this functional relation between R' and the corresponding R'' can be inverted. This yields an explicit expression, which enables straightforward computation of the actual sample reflectance, $R_{sam}(\lambda)$ from provisional DRS data, $R'(\lambda)$.
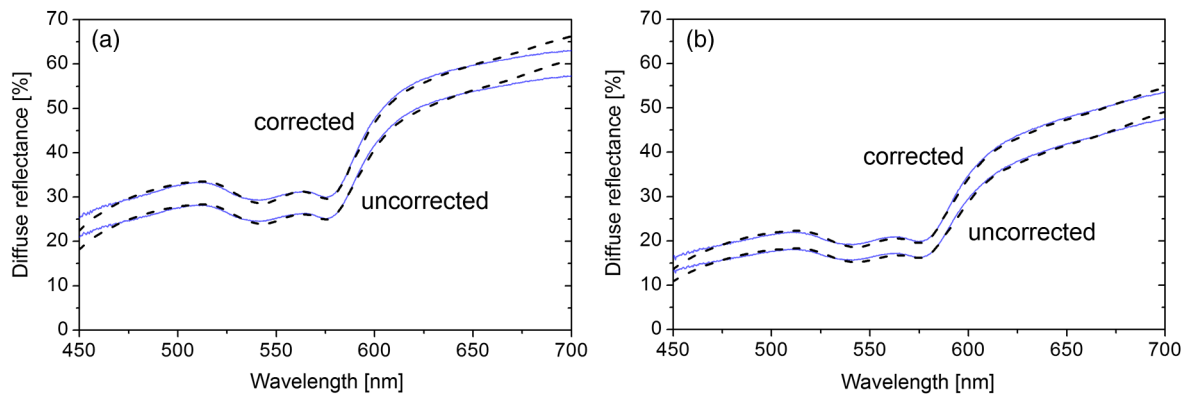
Fig. 6 Uncorrected and corrected DRS spectra as measured in (a) untanned and (b) tanned human skin (solid lines). Dashed lines indicate the best fits of diffusion approximation solutions for a two-layer skin model.

$$R_{sam}(\lambda) = R_{wh} R'(\lambda) \frac{1 - (1 - F)\rho}{1 - (1 - F)\rho - fR_{wh}[1 - R'(\lambda)]}.$$

(17)

If, for whatever reason, the experimentally observed relationship between R' and R'' should deviate from the functional dependence allowed by Eq. (16), one could approximate the first with any suitable function. Inverting this function then provides a closed expression for conversion of provisional DRS to SBSE-free data, $R''(\lambda)$. As a last resort, even if this function was noninvertable, one could still use the latter to prepare a look-up table to be used to the same effect. After having obtained $R''(\lambda)$, a simple multiplication with R_{wh} yields the correct sample reflectance, $R_{sam}(\lambda)$.

According to our analysis, the relationship between R' and R'' should be unique as long as both ρ and R_{wh} are constant within the involved spectral range. Under such circumstances, this functional dependence—even if deviating somewhat from Eq. (14)—includes all the information required for computational elimination of the SBSE. Following the approaches discussed in this subsection could, thus, eliminate the need to acquire any additional calibration data during (or preceding) each DRS measurement session.

Given that the discussed relationship depends exclusively on equipment specifics, rather than properties of particular samples, every user of the same DRS hardware should obtain the same correction function. It would, thus, make sense that the required instrument characterization be performed in advance by equipment manufacturers. Computational correction of provisional DRS data could then be integrated into acquisition software as an augmented calibration of the specific experimental setup.

5 Application Example

When using equipment that exhibits a significant SBSE, any quantitative analysis based on uncorrected DRS values may be prone to substantial systematic errors. In the following, we illustrate this point by one application example involving extraction of three tissue characteristics from experimental DRS.

Figure 6 presents DRS of healthy skin as measured on the forearm of a human volunteer with light complexion using the above described equipment. The provisional data, obtained by following the customary measurement procedure, and DRS corrected according to Eq. (7) are plotted for comparison (solid lines; note the labels). Figures 6(a) and 6(b) correspond to measurements at the same test site before and 1 week after extensive sun tanning, respectively.

The dashed lines indicate the respective best fits of analytical solutions derived earlier for a two-layer tissue model within the diffusion approximation.[34] Specifically, relative volume fractions of melanin in the 80 μm thick superficial layer (representing the epidermis) and blood in the semi-infinite layer underneath (dermis), as well as blood oxygen saturation were optimized for best match with experimental DRS between 450 and 600 nm. (The rationale behind this decision and other related details can be found in Refs. 35 and 36.) The absorption spectra of melanin and bloodless skin were taken from Jacques.[37] Absorption of blood was computed from spectra for oxygenated and deoxygenated hemoglobin.[38] Scattering in skin was modeled as a combination of Rayleigh and Mie scattering.[39]

A comparison of parameter values extracted from corrected versus uncorrected DRS (Table 1) confirms that presence of SBSE in the latter induces significant errors. In the case of

Table 1 Comparison of tissue characteristics as assessed by fitting analytical predictions to the corrected and uncorrected diffuse reflectance spectra (DRS) in Fig. 6. The last row presents relative deviations of the latter with respect to the former values. For each involved parameter, the left and right columns correspond to the values assessed from data in Figs. 6(a) and 6(b), respectively.

	Epidermal melanin (vol. %)		Dermal blood (vol. %)		Oxygen saturation (%)	
Corrected DRS	2.2	3.4	1.0	2.1	58	54
Uncorrected DRS	2.7	4.1	1.4	2.9	53	47
Relative error	+23%	+20%	+40%	+38%	−9%	−13%

untanned skin, fractional contents of epidermal melanin and dermal blood assessed from uncorrected DRS are overestimated by 23 and 40%, respectively, if the results obtained from the corrected spectra are taken as a reference. Meanwhile, oxygen saturation in the same test site is underestimated by 9%.

Analysis of the DRS measured in the same volunteer after sun tanning (right columns) shows that the artifacts induced by SBSE are very similar to those described above, despite the significant changes in epidermal melanin and dermal blood contents. Monitoring of seasonal changes in skin using the approach outlined above was presented elsewhere.[36]

6 Discussion

Our analysis of SBSE utilizes the reference port, which enables monitoring of light field inside the IS. The presented experimental example involving a common experimental setup shows that the fluence rate inside the IS can alter by up to 20% upon the substitution of white standard with the sample [Fig. 3(a)]. Because this effect is not accounted for in the customary measurement procedure, this leads to distortion of obtained DRS, known as SBSE [Fig. 3(b), Eq. (4)].

With the discussed experimental setup, Δ_{SBS} exceeds 5 percentage points at sample reflectance values between 30 and 72%. In this range, which includes reflectance values of fair human skin in red and near-infrared part of the spectrum, relative error of the provisional reflectance values R', thus, amounts from 7 to 17%.

As we demonstrate in this paper, two additional measurements performed at the reference port (of the white standard and a test sample, respectively) enable rigorous elimination of SBSE from provisional DRS. To the best of our knowledge, such an approach to elimination of SBSE was not documented in any earlier report.

Between the two presented experimental approaches, the one discussed in Sec. 3.2 has several practical advantages. It, namely, allows users to perform each pair of sample measurements with a minimal time interval and no need to reposition the IS between them. In addition, the port calibration term $\tilde{C}(\lambda)$ can be assessed only once for each experimental setup. All this reduces the total data acquisition time and lowers the risks of measurement artifacts, while at the same time allowing improved signal-to-noise ratios of corrected DRS.

We would like to propose that the presented approaches for experimental elimination of SBSE be supported in future versions of commercial DRS measurement software. This would enable users to characterize their specific setups and, if necessary, eliminate the SBSE within the acquisition software, instead of having to postprocess the data in separate programs.

In addition, since every user of the same IS and white standard material should obtain an identical port calibration term $\tilde{C}(\lambda)$ [Eq. (9)], the latter could be determined in advance by the equipment manufacturer and made available within the DRS measurement software.

However, even with such software support, users would still have to reposition the optical fiber between the signal and reference ports in order to perform each DRS measurement. This exposes the hardware, operators, as well as test subjects to additional stress. In our opinion, the optimal solution to this problem would be development of a dual-channel DRS spectrometer. By implementing a dual line detector and ability to have two optical fibers attached to the entrance slit, such an instrument would simultaneously acquire spectra at the IS signal and reference ports. The measurement protocol would, thus, remain identical to the customary one, yet yielding SBSE-free DRS. As a partial (or interim) solution, manufacturers could provide software support for those users who would choose to achieve the same effect by using two customary spectrometers connected in parallel to the IS signal and reference ports.

An alternative, albeit less elegant, hardware solution would involve implementation of an optical switch inside the IS housing. The switch (e.g., a movable mirror) would direct the signals collected at either the signal or reference port into a single optical fiber connected to a customary spectrometer. Four acquisitions would still be required to obtain each corrected DRS, but repositioning of the optical fiber between the two IS ports would no longer be required.

When $\rho(\lambda)$ and $R_{wh}(\lambda)$ exhibit a weak spectral dependence, which is the norm within the visible and near-infrared part of the spectrum, the theoretically predicted SBSE behavior matches our experimental observations very well (Fig. 5). This offers a possibility for computational elimination of SBSE, thus eliminating the need to perform any additional calibration measurements during the actual application. We have outlined several variations of this approach, utilizing either Eq. (17), another suitable analytical function, or a look-up table.

Since the functional relation between R' and the corresponding R'' [e.g., Eq. (16)] depends exclusively on equipment specifics, it would be best determined by equipment manufacturers. Computational correction of provisional DRS data could then be integrated into the acquisition software, essentially constituting an augmented calibration step. Note that unlike the experimental approaches discussed further above, this method could also be applied for approximate removal of the SBSE in IS without the reference port.

In applications where experimental DRS are used as input for subsequent quantitative analysis, presence of SBSE may induce substantial artifacts in the results. In the presented application example involving quantitative analysis of human skin, failure to remove SBSE resulted in overestimation of the fractional contents of epidermal melanin and dermal blood by 20 to 23% and 38 to 40%, respectively (Table 1). At the same time, the oxygen saturation level was underestimated by 9 to 13%. While these numbers may vary some more with sample specific (e.g., epidermal thickness, melanin, and blood content), general trends in terms of over- or undershooting of a given variable are, in our experience, quite universal.

To the best of our knowledge, the influence of SBSE on DRS measured with IS was not accounted for in any reported biomedical application. Based on the above evidence, it seems plausible that the related artifacts may be responsible for some of the discrepancies in the values of tissue optical properties, typical chromophore concentrations, etc., found in the literature. For example, several studies based on DRS measured with IS reported oxygen saturation values in healthy human skin averaging at 38%.[12,21] Studies involving alternative experimental approaches, in contrast, regularly report values of 50 to 60% and often even higher than that.[5,40] The above discrepancy is in qualitative agreement with our observation that failure to account for SBSE results in underestimation of oxygen saturation (Table 1). In addition to the fact that the amplitude of the measurement artifact varies with equipment specifics [Eq. (14)], specifics of subsequent analysis may also amplify its influence on the results to different degrees.

Evidently, several other causes unrelated to SBSE may also contribute to the above and other similar discrepancies in the literature. Nevertheless, an increased level of awareness, combined with the practical procedures for elimination of SBSE presented here, may help resolve some of the controversies and improve compatibility of future data obtained with different experimental setups.

Acknowledgments

References

1. R. M. P. Doornbos et al., "The determination of in vivo human tissue optical properties and absolute chromophore concentrations using spatially resolved steady-state diffuse reflectance spectroscopy," *Phys. Med. Biol.* **44**(4), 967–981 (1999).
2. A. N. Yaroslavsky et al., "Optical properties of selected native and coagulated human brain tissues in vitro in the visible and near infrared spectral range," *Phys. Med. Biol.* **47**(12), 2059–2073 (2002).
3. R. Zhang et al., "Determination of human skin optical properties from spectrophotometric measurements based on optimization by genetic algorithms," *J. Biomed. Opt.* **10**(2), 024030 (2005).
4. A. N. Bashkatov et al., "Optical properties of human skin, subcutaneous and mucous tissues in the wavelength range from 400 to 2000 nm," *J. Phys. Appl. Phys.* **38**(15), 2543–2555 (2005).
5. S. H. Tseng et al., "Chromophore concentrations, absorption and scattering properties of human skin in-vivo," *Opt. Express* **17**(17), 14599–14617 (2009).
6. D. Yudovsky and L. Pilon, "Retrieving skin properties from in vivo spectral reflectance measurements," *J. Biophotonics* **4**(5), 305–314 (2011).
7. V. V. Barun and A. P. Ivanov, "Role of epidermis in the optics and thermal physics of human skin," *Opt. Spectrosc.* **107**(6), 909–916 (2009).
8. N. Rajaram et al., "Experimental validation of the effects of microvasculature pigment packaging on in vivo diffuse reflectance spectroscopy," *Lasers Surg. Med.* **42**(7), 680–688 (2010).
9. I. Fredriksson, M. Larsson, and T. Strömberg, "Accuracy of vessel diameter estimated from a vessel packaging compensation in diffuse reflectance spectroscopy," *Proc. SPIE* **8087**, 80871M (2011).
10. A. N. Bashkatov et al., "Optical properties of melanin in the skin and skin-like phantoms," *Proc. SPIE* **4162**, 219–226 (2000).
11. G. Zonios et al., "Melanin absorption spectroscopy: new method for noninvasive skin investigation and melanoma detection," *J. Biomed. Opt.* **13**(1), 014017 (2008).
12. G. N. Stamatas et al., "In vivo measurement of skin erythema and pigmentation: new means of implementation of diffuse reflectance spectroscopy with a commercial instrument," *Br. J. Dermatol.* **159**(3), 683–690 (2008).
13. L. L. Randeberg et al., "Methemoglobin formation during laser induced photothermolysis of vascular skin lesions," *Lasers Surg. Med.* **34**(5), 414–419 (2004).
14. N. Kollias, I. Seo, and P. R. Bargo, "Interpreting diffuse reflectance for in vivo skin reactions in terms of chromophores," *J. Biophotonics* **3**(1–2), 15–24 (2010).
15. I. V. Ermakov and W. Gellermann, "Dermal carotenoid measurements via pressure mediated reflection spectroscopy," *J. Biophotonics* **5**(7), 559–570 (2012).
16. E. Salomatina et al., "Optical properties of normal and cancerous human skin in the visible and near-infrared spectral range," *J. Biomed. Opt.* **11**(6), 064026 (2006).
17. T. Lister, P. Wright, and P. Chappell, "Spectrophotometers for the clinical assessment of port-wine stain skin lesions: a review," *Lasers Med. Sci.* **25**(3), 449–457 (2010).
18. S. H. Tseng et al., "Noninvasive evaluation of collagen and hemoglobin contents and scattering property of in vivo keloid scars and normal skin using diffuse reflectance spectroscopy: pilot study," *J. Biomed. Opt.* **17**(7), 077005 (2012).
19. M. Bohnert, R. Baumgartner, and S. Pollak, "Spectrophotometric evaluation of the colour of intra-and subcutaneous bruises," *Int. J. Legal Med.* **113**(6), 343–348 (2000).
20. V. K. Hughes, "The practical application of reflectance spectrophotometry for the demonstration of haemoglobin and its degradation in bruises," *J. Clin. Pathol.* **57**(4), 355–359 (2004).
21. L. L. Randeberg et al., "A novel approach to age determination of traumatic injuries by reflectance spectroscopy," *Lasers Surg. Med.* **38**(4), 277–289 (2006).
22. F. J. J. Clarke and J. A. Compton, "Correction methods for integrating-sphere measurement of hemispherical reflectance," *Color Res. Appl.* **11**(4), 253–262 (1986).
23. K. Grandin and A. Roos, "Evaluation of correction factors for transmittance measurements in single-beam integrating spheres," *Appl. Opt.* **33**(25), 6098–6104 (1994).
24. J. Workman and A. Springsteen, *Applied Spectroscopy: A Compact Reference for Practitioners*, 1st ed., Academic Press, San Diego (1998).
25. A. Springsteen, "A guide to reflectance spectroscopy," 1992, http://www.photonicsonline.com/doc/technical-guide-reflectance-spectroscopy-0001 (24 January 2014).
26. G. Bain, *Integrating Sphere Diffuse Reflectance Technology for Use with UV-Visible Spectrophotometry*, Thermo Fisher Scientific, Madison, Wisconsin (2007).
27. J. L. Taylor, "How to choose the correct size (60 mm vs. 150 mm) integrating sphere," 2010, http://pe.taylorjl.net/PE_Blog/?p=308 (2 February 2014).
28. J. M. Palmer, "Measurement of transmission, absorption, emission, and reflection," in *Handbook of Optics*, M. Bass, Ed., 2nd ed., Vol. 2, pp. 25.1–25.5, McGraw-Hill Professional, New York (1994).
29. V. P. V. Wallace et al., "Spectrophotometric assessment of pigmented skin lesions: methods and feature selection for evaluation of diagnostic performance," *Phys. Med. Biol.* **45**(3), 735–751 (2000).
30. Ocean Optics, "SpectraSuite® spectrometer operating software: installation and operation manual," 2009, http://www.oceanoptics.com/technical/SpectraSuite.pdf (2 February 2014).
31. Labsphere, "Reflectance materials and coatings," http://www.labsphere.com/uploads/technical-guides/a-guide-to-reflectance-materials-and-coatings.pdf (2 February 2014).
32. Labsphere, "Integrating sphere theory and application," http://www.labsphere.com/uploads/technical-guides/a-guide-to-integrating-sphere-theory-and-applications.pdf (2 February 2014).
33. Ocean Optics, "ISP-REF integrating sphere," http://www.oceanoptics.com/Products/ispref.asp (2 February 2014).
34. L. O. Svaasand et al., "Tissue parameters determining the visual appearance of normal skin and port-wine stains," *Lasers Med. Sci.* **10**(1), 55–65 (1995).
35. P. Naglič, "Determination of human skin structure using diffuse reflectance spectroscopy," MS Thesis (in Slovene language), FMF, University of Ljubljana (2013).
36. P. Naglič et al., "Applicability of diffusion approximation in analysis of diffuse reflectance spectra from healthy human skin," *Proc. SPIE* **9032**, 90320N (2013).
37. S. L. Jacques, "Skin optics," http://omlc.ogi.edu/news/jan98/skinoptics.html (2 February 2014).
38. W. G. Zijlstra, A. Buursma, and O. W. van Assendelft, *Visible and Near Infrared Absorption Spectra of Human and Animal Haemoglobin: Determination and Application*, VSP, Zeist (2000).
39. S. L. Jacques, "Optical assessment of cutaneous blood volume depends on the vessel size distribution: a computer simulation study," *J. Biophotonics* **3**, 75–81 (2010).
40. S. J. Matcher, M. Cope, and D. T. Delpy, "In vivo measurements of the wavelength dependence of tissue-scattering coefficients between 760 and 900 nm measured with time-resolved spectroscopy," *Appl. Opt.* **36**, 386–396 (1997).

Luka Vidovič has obtained his BS degree in physics from the University of Ljubljana in 2011. Since November 2011, he has been employed as a junior research assistant at Jožef Stefan Institute, where he is involved in research projects in biomedical optics and working on his PhD thesis. His research efforts focus on applications of pulsed photothermal radiometry and more recently also diffuse reflectance spectroscopy for quantitative characterization of human skin and cutaneous malformations.

Boris Majaron is senior staff member at Jožef Stefan Institute in Ljubljana, Slovenia. After having obtained his PhD in physics from University of Ljubljana in 1993, his research interests shifted gradually from laser physics and spectroscopy of solid-state laser materials to biomedical optics, specifically laser ablation and characterization of biological tissues using pulsed photothermal radiometry and diffuse reflectance spectroscopy. He is a member of the editorial board for *Lasers in Surgery and Medicine*.